JOURNAL OF MATERIALS SCIENCE 26 (1991) 2566–2572

Crystallization of nanometre-size coprecipitated $PbTiO_3$ powders

G. R. FOX, E. BREVAL, R. E. NEWNHAM
Materials Research Laboratory, The Pennsylvania State University, University Park, PA 16802, USA

Crystallization of coprecipitated $PbTiO_3$ powder was studied by calcining as-precipitated powders at 400–800 °C for up to 262 h. The coprecipitated powders were prepared from a solution containing a 1:1 molar ratio of $Pb(NO_3)_2$:$TiCl_4$ and a 1.1:1 molar ratio of H_2O_2:$TiCl_4$. The solution containing the lead and titanium complexes was slowly added to NH_4OH solution under constant pH (10.00 ± 0.05) conditions that induced precipitation. Transmission electron microscopy and X-ray diffraction indicated that the calcined powders consisted of an intimate mixture of amorphous, cubic (or distorted tetragonal with $c_0/a_0 < 1.01$), and tetragonal ($c_0/a_0 = 1.065$) $PbTiO_3$ particles between 10 and 400 nm, with both particle size and phase content depending on heat treatment. Powders exhibiting the cubic or distorted tetragonal phase consisted of particles between 20 and 200 nm in diameter. Fully crystalline tetragonal $PbTiO_3$ powders consisting of 100–400 nm particles were prepared.

1. Introduction

The purpose of this study was to observe the particle size, morphology, and crystallization behaviour of coprecipitated $PbTiO_3$ powders. Previous reports on coprecipitated $PbTiO_3$ have described the coprecipitation process [1, 2] and the dielectric properties [3, 4] but little work has been completed on the crystallization behaviour of coprecipitated $PbTiO_3$. Because the amorphous as-precipitated powders and the calcined crystalline powders display extremely high surface areas [1, 2], it was of particular interest to determine whether a cubic $PbTiO_3$ phase is formed in calcined powders due to effects of particle size upon the cubic to tetragonal transformation energies.

In previous work on sol–gel derived $PbTiO_3$ [5], it was reported that an intermediate cubic phase is formed during the amorphous to tetragonal transformation but it is unclear whether the cubic phase is related to the small particle size of the powders. For $PbTiO_3$ prepared by the alkoxide method, a shift in the cubic to tetragonal transition temperature (T_c) toward lower temperatures was reported for particle sizes below 50 nm [6]. One group of workers have also reported stabilization of a distorted cubic $PbTiO_3$ phase for 20 nm powders prepared by the alkoxide method [7].

It has been suggested [8] that the decrease in T_c with decreasing particle size is due to an increase in pressure on the volume of the particle. This explanation assumes that the pressure on the volume is due to an "effective" surface tension and that the Laplace equation, given by

$$P = \frac{2\delta}{r} \quad (1)$$

where δ is the surface tension, and r the radius of the particle, is valid for a solid. Such a model also assumes that the shift in T_c is due only to pressure effects such as those reported by Sumara [9].

A second approach to interpreting the shift in T_c with size comes from the calculations of Batra *et al.* [10], on ferroelectric thin films. In this model, the stability of the ferroelectric phase is lowered because of depolarization fields which arise from incomplete charge compensation at the ferroelectric surface. For free ferroelectric particles in air, complete charge compensation at the particle surface is not likely. Hence, depolarization fields will increase and the stability of the ferroelectric phase will decrease with decreasing particle size.

Both of these models predict room-temperature stabilization of the cubic non-ferroelectric state below a critical particle size, but some factors are not considered which could greatly effect this size dependence. Both models assume single domain states for the ferroelectric phase. The effects of lattice defects, which may significantly contribute to the free energy of a small particle, are also ignored.

In this paper we present evidence for a possible cubic phase in fine-particle coprecipitated $PbTiO_3$. Transmission electron microscopy (TEM) can be used to differentiate between, cubic (Pm3m) and tetragonal (P4mm) $PbTiO_3$ phases by comparing convergent beam electron diffraction (CBED) patterns of individual powder particles. Because $PbTiO_3$ exhibits a large difference between the a_0 and c_0 unit cell parameters ($c_0/a_0 = 1.065$), the two-fold symmetry along tetragonal ⟨1 0 0⟩ can easily be identified by measuring the distance between the 1 0 0 and 0 0 1 spots of the CBED pattern (see Fig. 1). With a powder that

0022–2461/91 $03.00 + .12

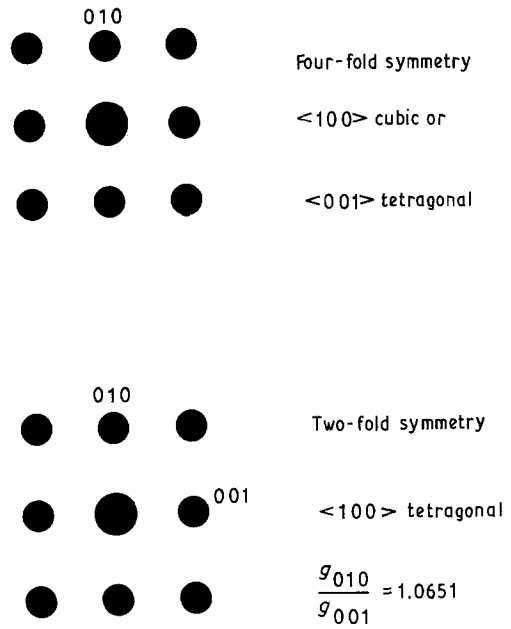

Figure 1 Calculated appearance of CBED patterns from simple zone axes in cubic and tetragonal $PbTiO_3$. For the tetragonal lattice $c/a = 1.0651$ will appear in the $\langle 100 \rangle$ CBED pattern as $g_{010}/g_{001} = 1.0651$.

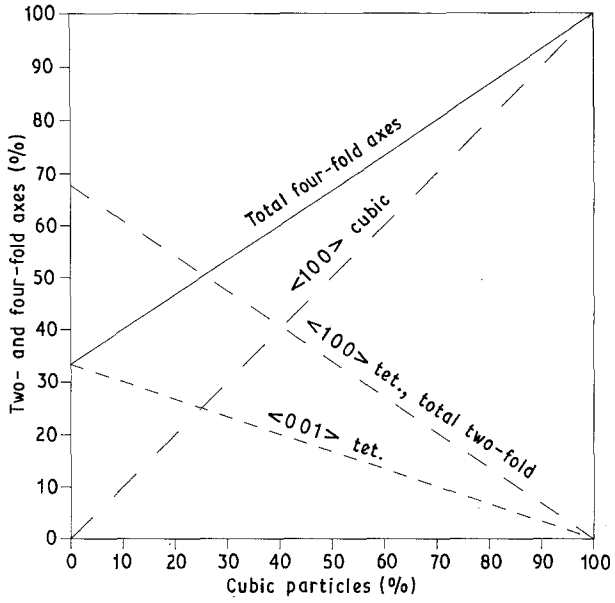

Figure 2 Probability for observing two- and four-fold $\langle 001 \rangle$ and $\langle 100 \rangle$ CBED patterns in a system containing cubic and tetragonal phases.

contains both cubic and tetragonal phases, the fraction of each phase can be determined by observing the CBED patterns of a large number of powder particles along $\langle 100 \rangle$ or $\langle 001 \rangle$ axes. Fig. 2 shows the expected percentage of two- and four-fold CBED patterns versus number fraction for powders containing both cubic and tetragonal particles. Using TEM with other supportive experimental techniques, it is possible to determine the particle size, shape and phase content of coprecipitated $PbTiO_3$ as a function of calcination time and temperature.

2. Experimental procedure

Fig. 3 outlines the preparation of coprecipitated $PbTiO_3$ powders. Hydrogen peroxide (30% by weight solution in water) was added to 14.15 ± 0.02 ml $TiCl_4$ solution ($2.65\ mol\,l^{-1}$) in à 1.1:1 molar ratio of H_2O_2:$TiCl_4$. The mixture was then diluted with deionized water to give 1000 ml solution and 37.50 ± 0.02 ml $Pb(NO_3)_2$ solution ($1.00\ mol\,l^{-1}$ concentration) was added to give a 1:1 ratio of $Pb(NO_3)_2$:$TiCl_4$. Deionized water was added to the mixed solution to give a final volume of 1500 ml solution. The solution was maintained at 43 ± 2 °C and constantly stirred. Precipitation was induced by pumping the heated solution at $10\ ml\,min^{-1}$ into a three-neck flask containing NH_4OH solution. Ammonium hydroxide solution was added to the three-neck flask simultaneously with the $Pb(NO_3)_2/TiCl_4$ solution to maintain the pH in the flask at 10.00 ± 0.05. The solution and precipitate formed in the three-neck flask was stirred constantly and the temperature was maintained at 43 ± 2 °C. After adding all the $Pb(NO_3)_2/TiCl_4$ solution to the three-neck flask, the precipitates were filtered and washed with deionized water to remove Cl^- and NO_3^- (less than 0.1 mol % of each species remained after washing).

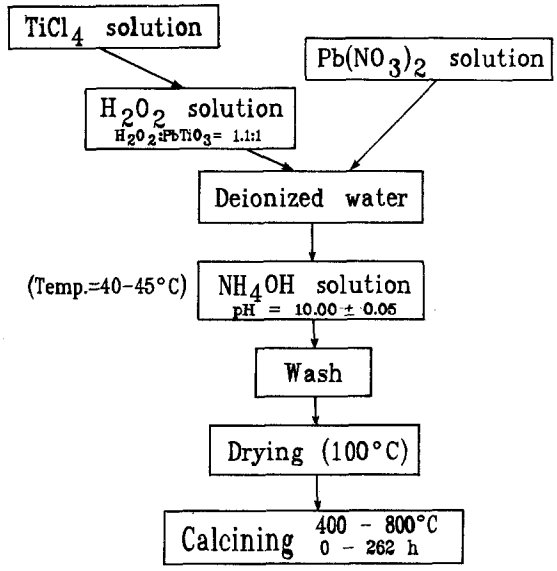

Figure 3 Diagram for $PbTiO_3$ coprecipitation process.

Concentrations of lead and titanium in the wash solutions were also monitored in order to confirm that neither lead nor titanium was leached from the precipitate. The precipitates were dried at 100 °C and crushed to form a powder. Samples of 3 g of the dried as-precipitated powders were calcined at 400–800 °C for 0–260 h in covered alumina crucibles.

The phase content of the calcined powders was determined by X-ray diffraction using CuK_α radiation at a scan rate of $1°\ 2\theta\ min^{-1}$. Integrated diffraction peak areas were obtained using a scan rate of $0.1°\ 2\theta\ min^{-1}$. All samples for X-ray diffraction were back-loaded packed powder specimens. The specific surface area of each powder was measured by a nitrogen single-point adsorption technique. Transmission electron microscopy (TEM, 120 kV) with energy dispersive spectroscopy (EDS) was used to investigate powder particle size, morphology, and composition.

The crystallographic structure of particles was determined using CBED (20 and 40 nm probe) and selected-area electron diffraction (SAED). TEM specimens were prepared from dilute suspensions of $PbTiO_3$ powders in isopropanol. A drop of the suspension was placed on a carbon-coated copper grid, dried, and carbon coated.

3. Results and discussion

X-ray diffraction data of the as-precipitated powders and powders calcined at 400 °C are presented in Fig. 4. The as-precipitated powder is amorphous as indicated by the broad peak at $d = 0.30$ nm. Crystalline $PbTiO_3$ peaks are not observed in powders calcined at 400 °C until they have been heat treated for 262 h. Powders calcined at 500 °C exhibited crystalline $PbTiO_3$ peaks after 2 h at temperature (see Fig. 5). For powders calcined above 500 °C, the diffraction patterns were similar to the pattern at 500 °C for 262 h.

A few of the diffraction patterns indicate that both amorphous and crystalline $PbTiO_3$ are present simultaneously as is demonstrated by the pattern for the sample heated at 400 °C for 262 h. In order to quantify the fraction of crystalline $PbTiO_3$ present in each of the calcined powders, the integrated 1 1 1 peak intensities were measured and normalized to the integrated 1 1 1 peak intensity measured for a standard coprecipitated powder calcined at 800 °C for 262 h. The concentration of crystalline $PbTiO_3$ increases markedly with increasing calcination temperature and time as shown in Fig. 6. Fully crystalline tetragonal $PbTiO_3$ is obtained only for powders calcined at 800 °C.

Specific surface area as a function of calcination time and temperature is shown in Fig. 7. At 400 and 500 °C, the specific surface area decreases with increasing calcination time, indicating an increase in particle size and/or density. At 600 °C, the specific surface area remains constant. A small decrease in specific surface area with increasing calcination time is observed again at 800 °C, suggesting further increase in particle size or density.

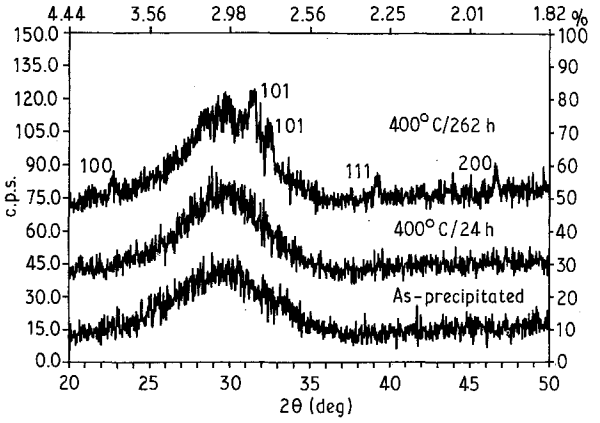

Figure 4 X-ray diffraction patterns indicating amorphous nature of as-precipitated powders and powders calcined at 400 °C for 24 h. Powder calcined at 400 °C for 262 h exhibits tetragonal $PbTiO_3$ peaks.

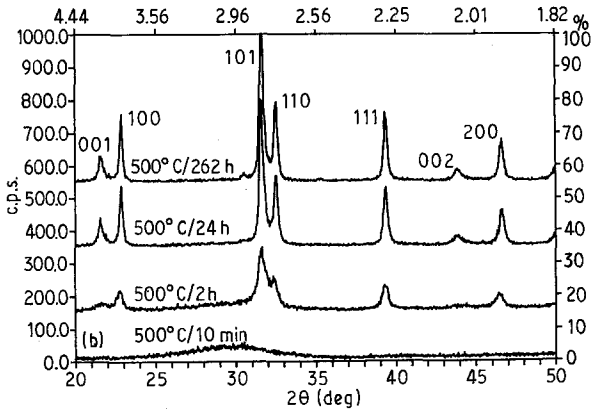

Figure 5 X-ray diffraction pattern of powder calcined at 500 °C for 10 min exhibits an amorphous structure while powders calcined for longer times show tetragonal $PbTiO_3$ peaks.

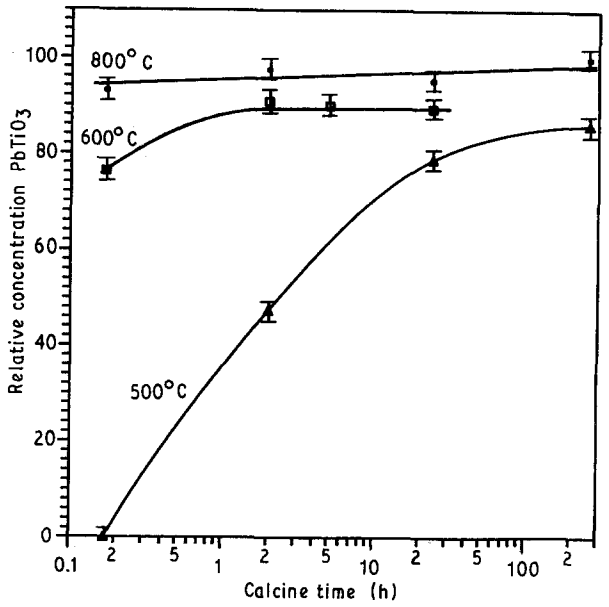

Figure 6 Relative concentration of crystalline $PbTiO_3$ as a function of calcination time and temperature.

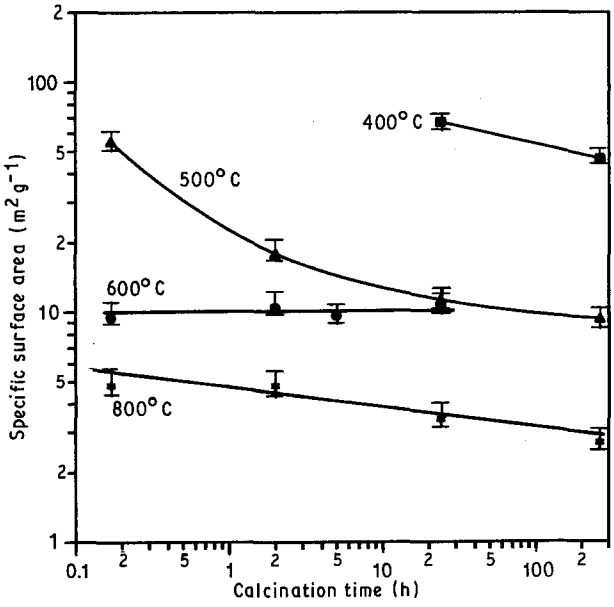

Figure 7 Specific surface area of calcined powders as a function of calcination time and temperature.

TABLE I Phase content and particle size of calcined powders

Calcination temp. (°C)	Calcination time (h)	% Amorphous phase (± 10%)	Cubic phase	Tetragonal phase
400	24	100 (10 nm)		
400	262	95 (10–20 nm)	yes (20–50 nm)	yes (50–100 nm)
500	0.2	85 (10–50 nm)	yes (20–50 nm)	
500	2	70 (20–50 nm)	yes (20–50 nm)	yes (50–100 nm)
500	24	15 (10–20 nm)	yes (20–75 nm)	yes (100–200 nm)
500	262	0		yes (100–200 nm) (elongated)
600	0.2	50	yes (50–100 nm)	yes (50–100 nm)
600	2	15		yes (100 nm)
600	24	0		yes (100 nm)
800	0.2	0		yes (100–200 nm) (elongated)
800	2	0		yes (150–200 nm) (elongated)
800	24	0		yes (200–300 nm) (elongated)
800	262	0		yes (200–400 nm) (aggregated)

TEM analysis of the powders provides further insight into the crystallization processes occurring during calcination (see Table I). As-precipitated powders exhibit particle sizes less than or approximately equal to 10 nm diameter, but the primary particles are highly agglomerated as shown in Fig. 8. Electron diffraction indicates that powders calcined at 400 °C for 262 h and at 500 °C and higher temperatures consist of combinations of crystalline and amorphous particles. The fraction of crystalline and amorphous particles depended upon calcination time and temperature, in agreement with the X-ray diffraction results. Examples of CBED patterns for crystalline single particles are shown in Fig. 9a and b. Fig. 9a shows a four-fold symmetry axis of either a tetragonal or cubic particle while Fig. 9b shows the two-fold symmetry axis of a tetragonal particle. Some powders calcined below 800 °C exhibited more four-fold symmetric CBED patterns than would be expected statistically for a purely tetragonal material (as indicated in Fig. 1). Because it is difficult to distinguish c_0/a_0 ratios of less than 1.01 in these CBED patterns, some apparent four-fold symmetry patterns may be two-fold patterns of tetragonal particles with $c_0/a_0 < 1.01$. Hence, the partially crystallized powders consist of a tetragonal phase with $c_0/a_0 = 1.065$ and a cubic phase or tetragonal phase with $c_0/a_0 < 1.01$.

Powders calcined at 500 °C for 10 min consist mostly of amorphous particles (as confirmed by X-ray and electron diffraction), but some groups of crystalline particles were observed as shown in Fig. 10. The

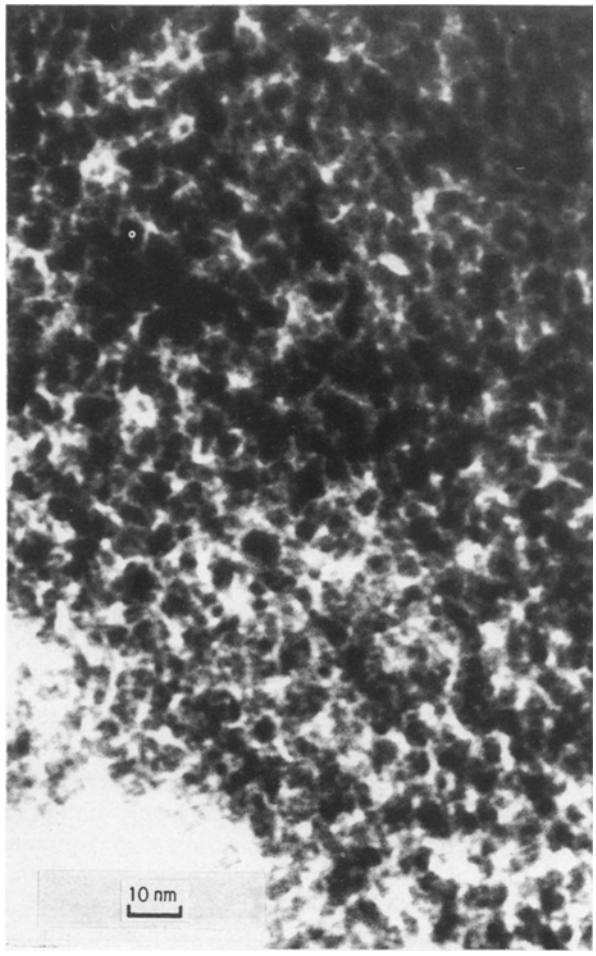

Figure 8 Amorphous as-precipitated $PbTiO_3$ precursor powder.

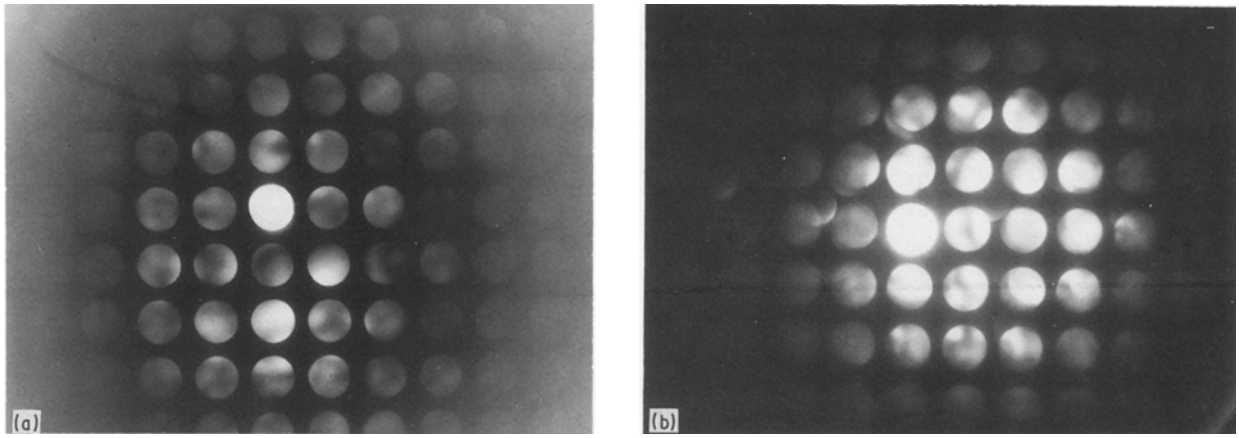

Figure 9 CBED patterns of single particles in calcined powders. (a) Cubic ⟨1 0 0⟩ direction or tetragonal ⟨0 0 1⟩ direction, (b) tetragonal ⟨1 0 0⟩ with a 1.06 ratio between the vertical and horizontal spots.

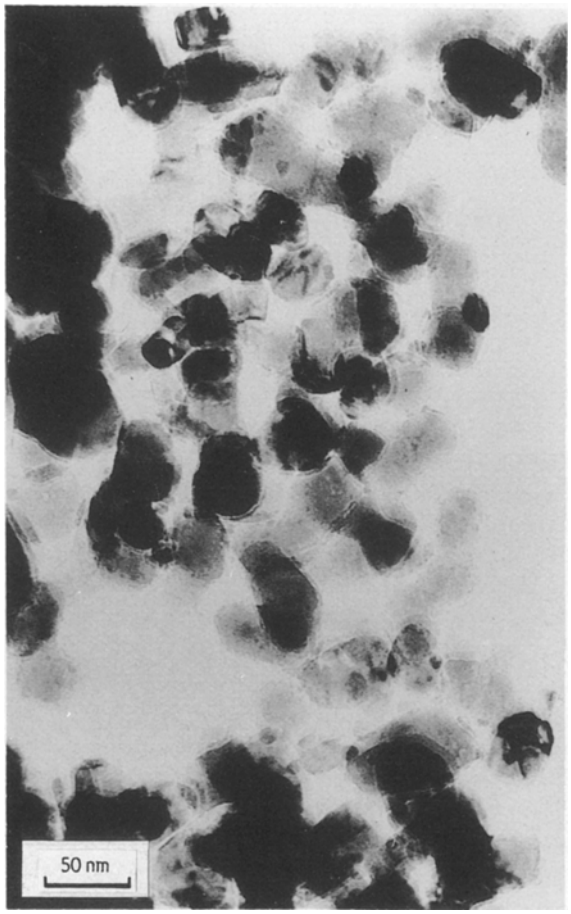

Figure 10 Crystalline particles that exhibit only four-fold symmetry along ⟨0 0 1⟩ or ⟨1 0 0⟩ axes in powders calcined at 500 °C/10 min.

crystalline particles are equiaxed and are approximately 20–50 nm diameter. All ⟨1 0 0⟩ or ⟨0 0 1⟩ CBED patterns of crystalline particles exhibited four-fold symmetry, thus indicating a cubic phase or tetragonal phase with $c_0/a_0 < 1.01$.

The crystalline particles in powders calcined at 400 °C for 262 h and 500 °C for 2 h were similar to those shown in Fig. 10. These powders also contained large quantities of amorphous particles surrounding regions of crystalline particles. More four-fold than two-fold symmetry CBED patterns, for ⟨1 0 0⟩ or ⟨0 0 1⟩ directions, were observed for these powder particles. Further evidence indicating the presence of cubic or distorted tetragonal phases ($1.000 < c_0/a_0 < 1.065$) comes from asymmetry of the 0 0 2 and 2 0 0 X-ray diffraction peaks for the partially crystallized powders. Fig. 11a and b show the 0 0 2 and 2 0 0 diffraction peaks for fully crystallized powder calcined at 800 °C for 262 h and powder calcined at 500 °C for 2 h, respectively. By comparing the two patterns, one sees that the peaks in Fig. 11b are broadened asymmetrically. The 0 0 2 peak is broadened more on the high angle side while the 2 0 0 peak is broadened more on the low angle side. This is the type of diffraction pattern expected for a powder containing a distribution of particles with c_0/a_0 ratios between 1.000 and 1.065. Fig. 11b also shows an average $c_0/a_0 = d_{0\,0\,2}/d_{2\,0\,0} = 1.050$ which is slightly smaller than the $c_0/a_0 = 1.065$ for large-particle $PbTiO_3$ powders.

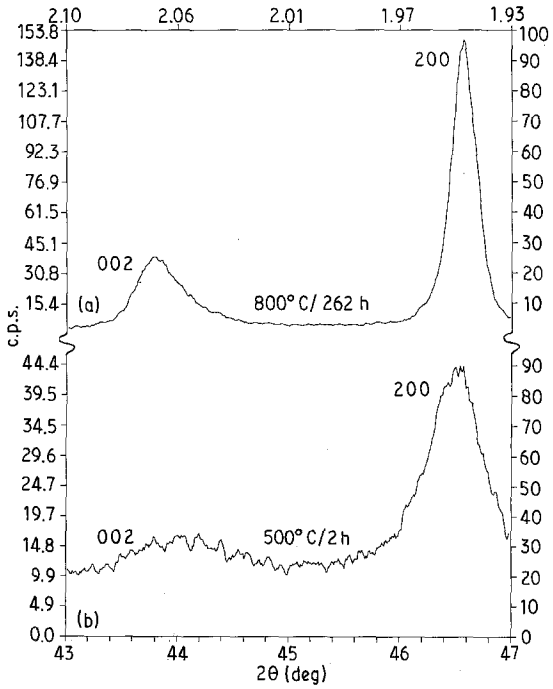

Figure 11 (a) 0 0 2 and 2 0 0 X-ray diffraction peaks for powder calcined at 800 °C/262 h, (b) asymmetrically broadened 0 0 2 and 2 0 0 peaks with average $c_0/a_0 = d_{0\,0\,2}/d_{2\,0\,0} = 1.050$ for powder calcined at 500 °C/2 h.

A micrograph of powder calcined at 500 °C for 24 h is shown in Fig. 12. Clusters of small amorphous particles are intimately mixed with larger crystalline particles. Necking between amorphous particles (10–30 nm), which was also observed in the powders discussed above, indicates that the amorphous particles sinter before crystallizing. Crystalline particles are 20–200 nm diameter and are generally equiaxed. Powders calcined at 600 °C for 10 min show similar quantities and morphologies of amorphous and crystalline material, but the crystalline particle sizes range from 50–100 nm. As shown by electron diffraction, both powders appear to contain a cubic phase or distorted tetragonal phase.

Fig. 13 is a micrograph of powder calcined at 600 °C for 2 h. A small number of amorphous clusters are found between the large crystalline grains. The amorphous clusters consist of 10–30 nm equiaxed particles. Crystalline particles are equiaxed, faceted and 20–100 nm diameter. Powders calcined at 500 °C for 262 h and 600 °C for 24 h exhibit crystalline particles like those shown in Fig. 13, but no amorphous particles were found.

At 800 °C only crystalline particles were observed as shown in Fig. 14. Both equiaxed and elongated particles were present. Particle sizes ranged from 100–200 nm for 10 min to 200–400 nm for 262 h calcination times. Particles also began to sinter at the longer calcination times.

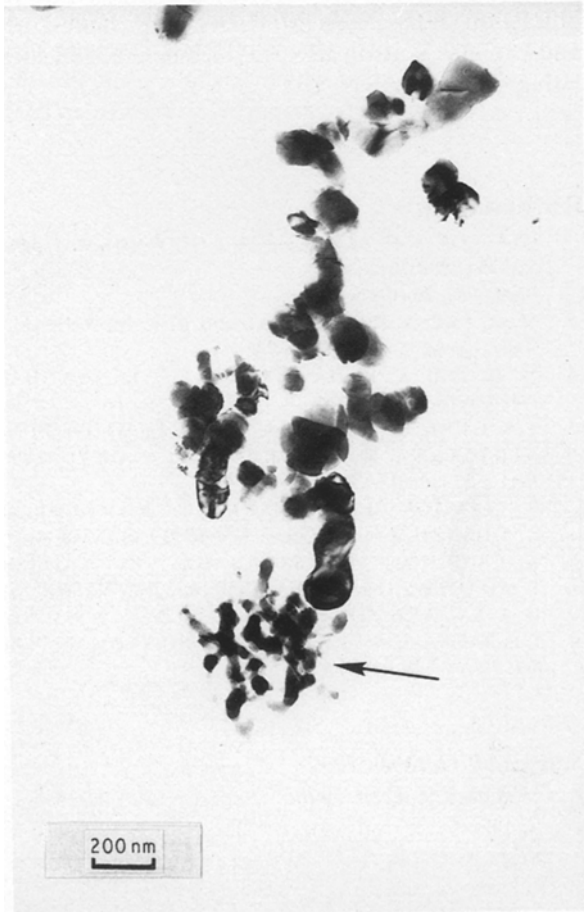

Figure 12 Cluster of sintered amorphous particles (arrowed) and 100–200 nm crystalline particles in powder calcined at 500 °C for 24 h.

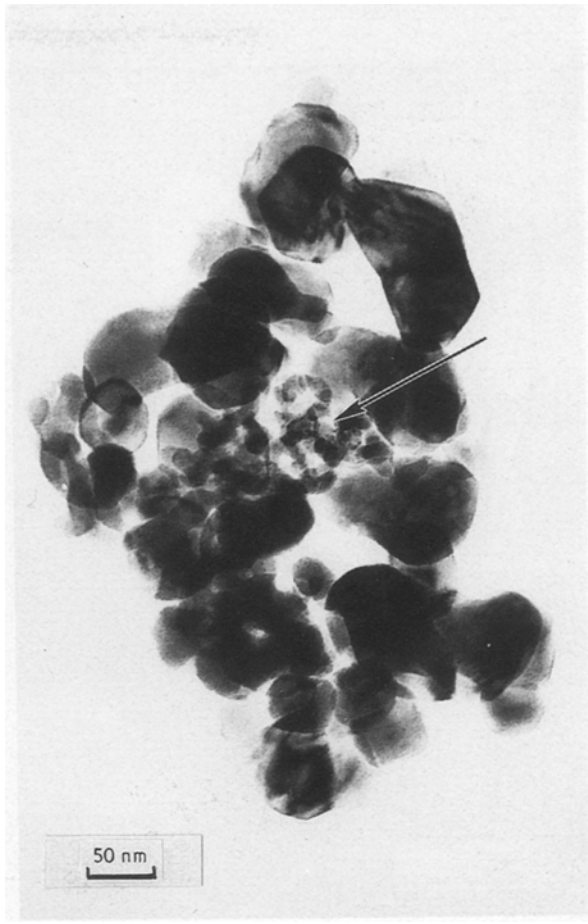

Figure 13 Small 10–30 nm amorphous particles (arrowed) between large 100 nm crystalline particles calcined at 600 °C for 2 h.

None of the SAED ring patterns or CBED patterns indicated the presence of $Pb_2Ti_2O_6$ or $PbTi_3O_7$ which are cubic structures that may possibly form within the calcined powders. Hence it was concluded that the powders exhibiting excessive amounts of four-fold axes contain cubic or distorted tetragonal ($c_0/a_0 < 1.01$) $PbTiO_3$. In all of the powders, especially those believed to contain a cubic $PbTiO_3$ phase, many of the small particles (≤ 100 nm) contained what appeared to be dislocations or other lattice defects. Such defects may have large effects upon the free energies of the crystalline phases, therefore causing the formation of a cubic phase. With extended heat treatments, such defects would be depleted along with any phases stabilized by such defects. By considering the phase information from both X-ray and electron diffraction, a phase formation diagram as a function of calcination time and temperature can be constructed as shown in Fig. 15. The broken lines used to separate phase fields signify that the exact position and shape of the boundaries have not been conclusively determined. Hence, the boundaries shown only indicate general trends in phase formation for increasing calcination time and temperature.

4. Conclusions

Crystallization of coprecipitated $PbTiO_3$ powders is complex in that several phases occur that are dependent upon heat treatment and particle size. Also, several

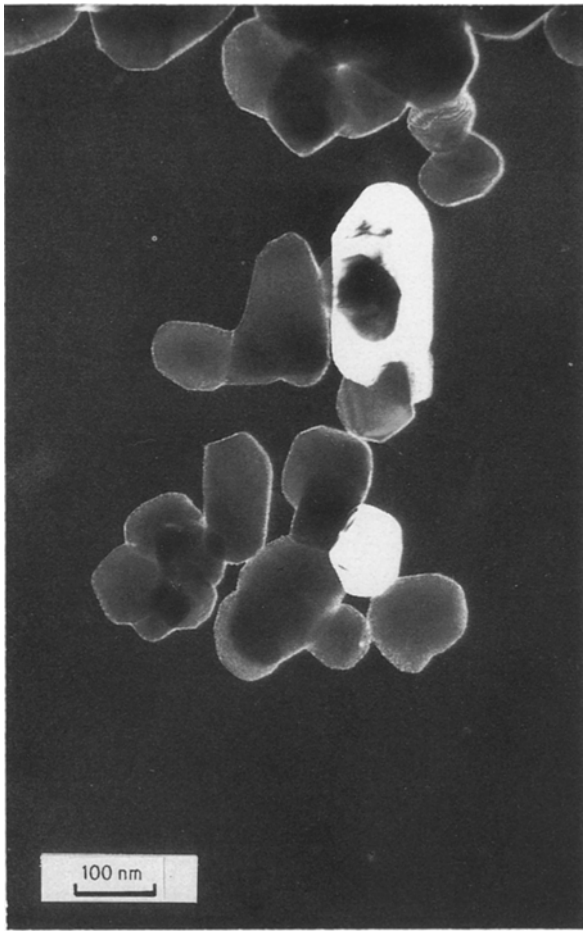

Figure 14 Elongated and sintered tetragonal $PbTiO_3$ particles calcined at 800 °C for 24 h.

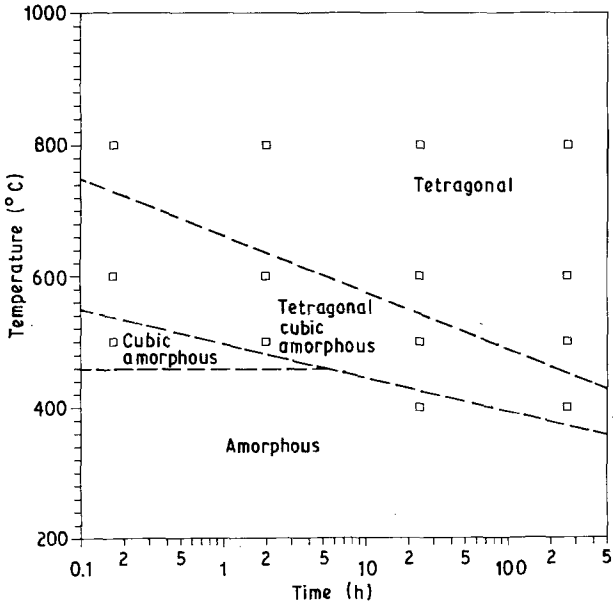

Figure 15 Formation diagram of $PbTiO_3$ phases as a function of calcination time and temperature. Dashed line boundaries indicate general trends and have not been determined exactly.

particle morphologies occur which are dependent upon heat treatment. As-precipitated amorphous powders exhibit equidimensional particles approximately 10 nm in size which sinter and grow to form equidimensional crystalline particles. Small equidimensional crystalline particles between 20 and 100 nm primarily show cubic or distorted tetragonal ($1.000 < c/a < 1.065$) symmetry. With increasing calcination time and temperature, equidimensional crystalline particles grow in size (50–200 nm) and transform to the tetragonal state (up to 400 nm). Further calcination causes necking between crystalline tetragonal particles along with particle growth, pronounced faceting, and particle elongation.

The reason for the appearance of a cubic $PbTiO_3$ phase at room temperature may be due to lattice defects, size effects, charge compensation effects or a combination of many factors arising from the boundary conditions imposed by nanometre-size particles. Investigations of materials containing higher quantities of cubic phases need to be completed before it can be determined which physical effects play a dominant role in stabilizing a room-temperature cubic $PbTiO_3$ phase.

Acknowledgements

The authors thank Ann Casciani who made the specific surface area measurements and Dr Clive Randall for discussions concerning the TEM and electron diffraction data. Susan McKinstry, Dr James Adair and Douglas Watson also provided helpful and stimulating discussion.

References

1. G. R. FOX, J. H. ADAIR and R. E. NEWNHAM, *J. Mater. Sci.* **25** (1990) 3634–3640.
2. *Idem., ibid.* **26** (1991) in press.
3. M. H. LEE, A. H. HALLIYAL and R. E. NEWNHAM, *J. Amer. Ceram. Soc.* **72** (1989) 986.
4. M. H. LEE, A. H. HALLIYAL and R. E. NEWNHAM, *Ferroelectrics* **87** (1988) 71.
5. S. R. GURKOVICH and J. B. BLUM, *ibid.* **62** (1985) 189.
6. K. ISHIKAWA, K. YOSHIKAWA and N. OKADA, *Phys. Rev. B* **37** (1988) 5852.
7. O. YAMAGUCHI, A. NARAI, T. KOMATSU and K. SHIMIZU, *J. Amer. Ceram. Soc.* **69** (1986) C-256.
8. K. UCHINO, E. SADANAGA, K. OONISHI, T. MOROHASHI and H. YAMAMURA, *ibid.* **72** (1989) 1555.
9. G. A. SAMARA, *Ferroelectrics* **2** (1971) 277.
10. I. P. BATRA, P. WURFEL and B. D. SILVERMAN, *J. Vac. Sci. Technol.* **10** (1973) 687.

Received 9 October 1989
and accepted 9 April 1990